Optical characterization of a $Cd_{0.85}Mg_{0.15}Se$ mixed crystal



2007 J. Phys.: Condens. Matter 19 266002

(http://iopscience.iop.org/0953-8984/19/26/266002)

IOP PUBLISHING JOURNAL OF PHYSICS: CONDENSED MATTER

J. Phys.: Condens. Matter **19** (2007) 266002 (8pp) doi:10.1088/0953-8984/19/26/266002

# Optical characterization of a $Cd_{0.85}Mg_{0.15}Se$ mixed crystal

**P J Huang[1], Y S Huang[1,4], F Firszt[2], S Łęgowski[2], H Męczyńska[2] and K K Tiong[3]**

[1] Department of Electronic Engineering, National Taiwan University of Science and Technology, Taipei 106, Taiwan
[2] Institute of Physics, N Copernicus University, Grudządzka 5/7, 87-100 Toruń, Poland
[3] Department of Electrical Engineering, National Taiwan Ocean University, Keelung 202, Taiwan

E-mail: ysh@mail.ntust.edu.tw

Received 14 February 2007, in final form 17 April 2007
Published 24 May 2007
Online at stacks.iop.org/JPhysCM/19/266002

**Abstract**

We present an optical characterization of a Bridgman-grown wurtzite-type $Cd_{0.85}Mg_{0.15}Se$ mixed crystal in the near-band-edge interband transitions using temperature-dependent contactless electroreflectance (CER) and photoreflectance (PR) in the temperature range 15–400 K. The interband excitonic transitions A and C originating from the band edge and spin–orbital splitting critical points of the sample, respectively, have been observed in the CER/PR spectra. The transition energies and broadening function of the excitonic features are determined via a lineshape fit to the CER/PR spectra. The parameters that describe the temperature dependence of the transition energies of excitons A and C, and the broadening function of exciton A, are evaluated and discussed.

## 1. Introduction

The Mg-based II–VI semiconductors have recently attracted much attention because of their potential applications in the field of blue–green light sources and other optoelectronic devices [1]. These alloy systems have the possibility of tuning the band gap and lattice constants by varying the Mg concentration so that they can easily be matched with III–V substrates. Considerable work has been devoted to the study of the device applications as well as to the physical properties of the Mg-based II–VI alloys [2–6]. Among the Mg-based II–VI alloy systems, however, $Cd_{1-x}Mg_xSe$ has not been studied more extensively than the other systems in spite of its suitability for optoelectronic device application in the range of the entire visible spectrum from the band gap 1.74 eV of CdSe to 4.0 eV of MgSe [7]. To date, only a few papers have been reported on the recombination processes in $Cd_{1-x}Mg_xSe$ crystals and the

[4] Author to whom any correspondence should be addressed.

fabrication of green-light-emitting structures using n-CdSe and p-ZnTe regions separated by a graded $Cd_{1-x}Mg_xSe$ injection region [1, 8].

This report deals with a detailed optical characterization of a wurtzite (WZ)-type $Cd_{0.85}Mg_{0.15}Se$ mixed crystal using contactless electroreflectance (CER) and photoreflectance (PR) in the temperature range 15–400 K. Room-temperature surface photovoltage spectroscopy (SPS) has been used as a technique for checking the surface condition of the sample. The mixed crystal was grown from the melt by the modified high-pressure Bridgman method. The transition energies and the broadening parameters of the A and C excitons originating, respectively, from the band edge and spin–orbital splitting were determined via a lineshape fit to the CER/PR spectra. The parameters that describe the temperature dependence of the interband transition energies of excitons A and C, and the broadening function of the A feature, are evaluated and discussed.

## 2. Experimental details

The $Cd_{0.85}Mg_{0.15}Se$ mixed crystal was grown from the melt by the high-pressure Bridgman method [9]. The CdSe (6 N Koch-Light) and Mg (purity 99.8%) powders were mixed and put into a graphite crucible. The crucible containing the mixture was kept for three hours at a temperature of 1600 K, and then moved out of the heating zone with a rate of 2.4 mm $h^{-1}$. An argon overpressure of 12 MPa was kept during the entire growth period. The crystal bar obtained was cut into plates of about 1.5 mm thickness, and mechanically polished. The structure and composition of the sample were determined by an x-ray method. X-ray investigations showed the crystal plates are uniform in composition and exhibit a single wurtzite phase or wurtzite as the main phase with admixture of another polytype [9].

It is emphasized that prior to any optical experimentation, the sample must be treated with further mechanical polishing and chemical etching process to remove mechanical defects on the surface. The sample was mechanically polished using successively finer abrasives with the final polishing process using 0.05 $\mu$m aluminium-oxide ($Al_2O_3$) powder. For optical measurements, the sample was additionally etched in a mixture of $K_2Cr_2O_7$:$H_2SO_4$:$H_2O$ with a proportion of 3:2:1 followed by a treatment in $CS_2$ and 50% NaOH solution [10].

The SPS measurements were done by using a metal–insulator–semiconductor (MIS) configuration with chopped light in air at room temperature. A static metal grid was used as a top electrode and the air gap between the metal grid and the sample was about 50 $\mu$m. The sample was mounted on a copper sample holder. A 150 W xenon arc lamp filtered by a Photon Technology Inc. 0.25 m monochromator provided the monochromatic light. The incident light intensity was maintained at a constant level of $10^{-5}$ W $cm^{-2}$. A beam splitter was placed in the path of the incident light. The intensity of this radiation was monitored by a power meter and was keep constant by a stepping motor connected to a variable neutral-density filter, which was also placed in the path of the incident beam. The chopping frequency was kept at 200 Hz. The induced surface photovoltage (SPV) on the metal grid was measured with a copper bottom as the ground electrode, using a buffer circuit and a lock-in amplifier. In CER an ac modulating voltage ($\sim$1 kV at 200 Hz) is applied between a front wire grid electrode and a second electrode consisting of a metal plate. These two electrodes are separated by an insulating spacer in such a manner that there is a very thin layer ($\sim$0.1 mm) of air (or vacuum) between the front surface of the sample and the front electrode. Thus, there is no direct contact with the front surface of the sample. The probe beam enters through the front wire grid. The reflected light was detected by a UV-enhanced silicon photodiode. The dc output of this silicon photodiode was maintained constant by a servo mechanism of a variable neutral-density filter. A dual-phase lock-in amplifier was used to measure the detected signals. In PR measurements,

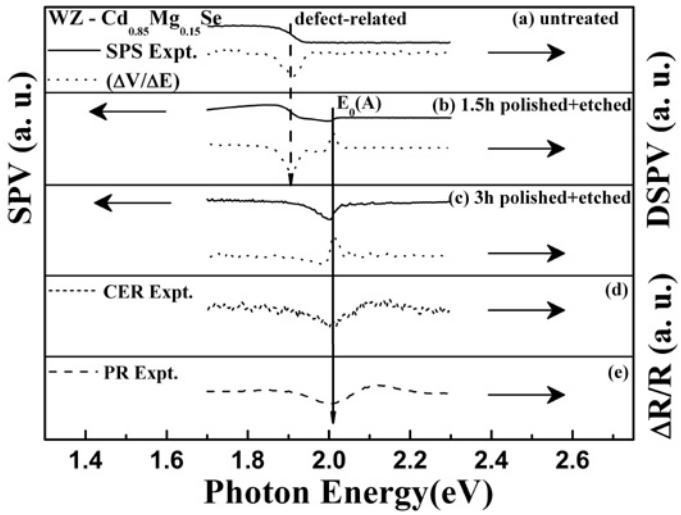


**Figure 1.** The SPS and numerically computed $(\Delta V/\Delta E)$ spectra of a WZ-type $Cd_{0.85}Mg_{0.15}Se$ mixed crystal (a) untreated, (b) polished and chemically etched for 1.5 h, (c) polished and chemically etched method for 3 h; (d) CER and (e) PR spectra for the damage-removed WZ-type $Cd_{0.85}Mg_{0.15}Se$ mixed crystal near-band-edge at 300 K.

the modulation of the built-in electric field is caused by photoexcited electron–hole pairs created by a mechanically chopped 325 nm line (∼1 mW) of a He–Cd laser. The modulating frequency is set at 200 Hz. The entire data acquisition procedure was performed under computer control. Multiple scans over a given photon energy range were programmed until a desired signal-to-noise level was attained. For temperature-dependent measurements, an RMC model 22 closed-cycle cryogenic refrigerator equipped with a digital thermometer controller was used for the low-temperature measurements. For the high-temperature experiments, the sample was mounted on one side of a copper finger of an electrical heater, which enabled one to control and stabilize the sample temperature. The temperature-dependent measurements were made between 15 and 400 K with a temperature stability of 0.5 K or better.

## 3. Results and discussion

As emphasized earlier, a proper surface treatment of the sample must be performed to eliminate the damaged layer formed on the surface caused by mechanical polishing. The SPS technique can be utilized to check the condition of the surface layer. The existence of such damage is revealed by the SPS spectra of the untreated and treated $Cd_{0.85}Mg_{0.15}Se$ mixed crystal, as depicted by the full curve in figures 1(a)–(c). The dotted curves in figures 1(a)–(c) represent, respectively, the numerically computed normalized first derivative of the surface photovoltage (DSPV) signal with respect to the photon energy $(\Delta V/\Delta E)$ of the untreated and treated sample. The SPV (DSPV) spectra of the as-received sample as depicted in figure 1(a) consist of a dominant defect-related broad feature in the energy range 1.85–1.95 eV. However, after surface treatment of 1.5 h of mechanical polishing followed by chemical etching, the SPV (DSPV) spectra showed an exciton line together with a significant reduction of the defect-related feature, as illustrated in figure 1(b). Figure 1(c) shows the SPV (DSPV) spectra of the sample with 3 h of mechanical polishing followed by chemical etching. After such a surface treatment process almost no surface defects can be detected from SPS, CER and PR measurements, as

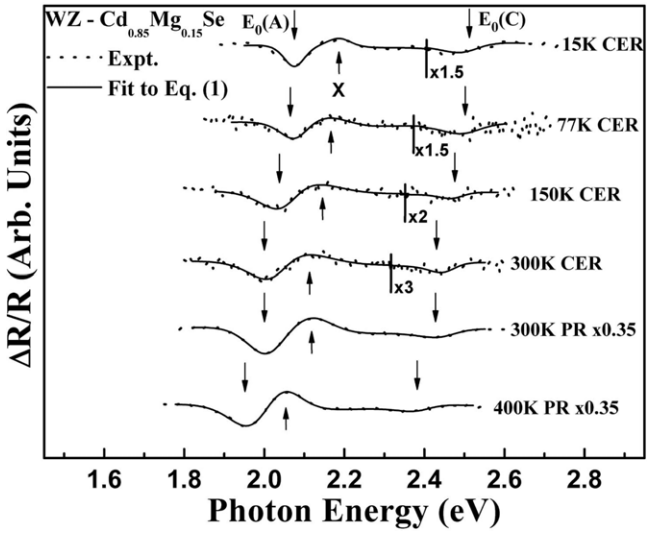


**Figure 2.** Experimental (dotted curves) CER/PR spectra of a WZ-type $Cd_{0.85}Mg_{0.15}Se$ mixed crystal at several temperatures between 15 and 400 K. The solid lines are least-squares fits to the first derivative of Lorentzian lineshape functional form. The obtained values of the energies are indicated by the arrows.

evidenced from the complete elimination of the defect-related feature, and only the exciton line is recorded. The energy position of the excitonic transition is estimated to be $2.002 \pm 0.005$ eV, and this agrees well with the subsequent CER and PR measurements, as shown in figures 1(d) and (e). Subsequently, CER/PR measurements performed for the damage-removed sample were checked by SPS.

Displayed by the dotted curves in figure 2 are the detailed experimental CER/PR spectra of a $Cd_{0.85}Mg_{0.15}Se$ mixed crystal at 15, 77, 150, 300 and 400 K. The full curves are least-squares fits to the first derivative of a Lorentzian lineshape function of the form [11, 12]

$$\frac{\Delta R}{R} = \mathrm{Re} \sum_{j=1} A_j e^{i\Phi_j} (E - E_j + i\Gamma_j)^{-n} \tag{1}$$

where $A_j$ and $\Phi_j$ are the amplitude and phase of the line shape, $E_j$ and $\Gamma_j$ are the energy and broadening parameter of the transitions, and the value of $n$ depends on the origin of the transitions. For the derivative functional form, $n = 2$ is appropriate for the bound states such as excitons [11]. The obtained values of $E_j$ are indicated by arrows in the figure.

As shown in figure 2, the CER spectrum of at 15 K shows three distinct features, as indicated by the vertical arrows. Their transition energies are determined to be $2.090 \pm 0.004$, $2.197 \pm 0.006$, and $2.521 \pm 0.006$ eV, respectively. As the temperature increases, the CER spectral features shift towards lower energies and broaden. The features on the lower-energy side are not clearly resolved at higher temperature. Nevertheless, the lineshape fit reveals that two features are required to describe the broadened structure well at higher temperature. The fitted values of the transition energies at 300 K are $2.001 \pm 0.006$, $2.105 \pm 0.008$, and $2.427 \pm 0.008$ eV, respectively. The obtained values of the lowest transition feature at 2.090 eV (15 K) and 2.001 eV (300 K) agree quite well with the photoluminescence (PL) results [10] which give the peak position of exciton line at 2.081 eV (40 K) and 2.011 eV (300 K). The value of 2.001 eV at 300 K also corresponds well to the transition energy of the A exciton at 1.999 eV

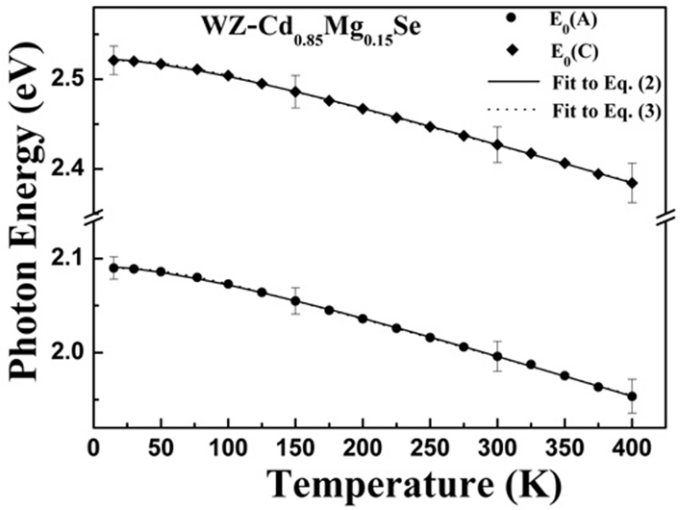


**Figure 3.** The temperature dependence of the transition energies for exciton A (solid circles) and exciton C (solid diamond) with representative error bars of a WZ-type $Cd_{0.85}Mg_{0.15}Se$ mixed crystal. The full curves and dotted curves, respectively, are least-squares fits to equations (2) and (3).

as determined by Firszt *et al* [10] from spectroscopic ellipsometric measurements performed at room temperature. They also reported the energy of the C exciton to be 2.429 eV, which is nearly identical to the position of the highest energy feature for the presently investigated sample. The work of Firszt *et al* [10] gives the energy separation of the A and C excitons to be 430 meV, which agrees well with the energy difference of 431 meV as evaluated from the present CER measurements for the lowest and the highest energy features. We can therefore assign the lowest energy feature to be the A exciton and the highest energy feature to be the C exciton. Turning our attention to the feature at 2.197 eV (15 K), denoted as X, we found that the energy separation between this second feature and exciton A is ∼107 meV; this is much larger than the room-temperature energy difference between A and B excitons of ∼40 meV for WZ-type CdSe [13]. Therefore, the assignment of the feature at 2.197 eV (15 K) as the B exciton may not be appropriate. The origin of this feature is not clear, and it is tentatively attributed to the coexistence of some other polytypic phases with wurtzite as the main phase in the Mg-containing crystal.

Plotted by the solid circles and solid diamonds in figure 3 are the temperature variations of the experimental values of $E_0^{\mathrm{A}}(T)$ and $E_0^{\mathrm{C}}(T)$, respectively, with the representative error bars for a WZ-type $Cd_{0.85}Mg_{0.15}Se$ mixed crystal. The full curves are least-squares fits to the Varshni semi-empirical relationship [14] as given by

$$E_0^j(T) = E_0^j(0) - \frac{\alpha_j T^2}{(\beta_j + T)}. \tag{2}$$

Here $j$ refers to either A or C exciton transitions, $E_0^j(0)$ is the energy at 0 K; $\alpha_j$ and $\beta_j$ are constants. The constant $\alpha_j$ is related to the electron (exciton)–average phonon interaction and $\beta_j$ is closely related to the Debye temperature. The values obtained for $E_0^j(0)$, $\alpha_j$ and $\beta_j$ are listed in table 1. For comparison, the parameters for the near-band-edge transition energies of WZ-type $Cd_{0.925}Be_{0.075}Se$ [15], WZ-type CdSe [13], zinc blende (ZB)-type ZnSe [16], and ZB-type $Zn_{0.56}Cd_{0.44}Se$ [16] are also listed in table 1.

**Table 1.** Values of the Varshni-type and Bose–Einstein-type fitting parameters, which describe the temperature dependence of the transition energies of excitons A and C of a WZ-type $Cd_{0.85}Mg_{0.15}Se$ mixed crystal. The parameters for WZ-type $Cd_{0.925}Be_{0.075}Se$, WZ-type CdSe, ZB-type ZnSe, and ZB-type $Zn_{0.56}Cd_{0.44}Se$ are included for comparison.

| Samples | Feature | $E(0)$ (eV) | $\alpha$ ($10^{-4}$ eV K$^{-1}$) | $\beta$ (K) | $a_B$ (meV) | $\Theta_B$ (K) |
|---|---|---|---|---|---|---|
| WZ-type $Cd_{0.85}Mg_{0.15}Se$[a] | $E_0$(A) | $2.090 \pm 0.004$ | $4.15 \pm 0.2$ | $217 \pm 30$ | $37 \pm 5$ | $184 \pm 30$ |
| | $E_0$(C) | $2.521 \pm 0.006$ | $4.07 \pm 0.3$ | $225 \pm 40$ | $42 \pm 8$ | $202 \pm 40$ |
| WZ-type $Cd_{0.925}Be_{0.075}Se$[b] | $E_0$(A) | $1.964 \pm 0.003$ | $4.02 \pm 0.1$ | $210 \pm 20$ | $34 \pm 4$ | $185 \pm 20$ |
| | $E_0$(C) | $2.398 \pm 0.003$ | $3.92 \pm 0.1$ | $220 \pm 30$ | $38 \pm 7$ | $200 \pm 30$ |
| WZ-type CdSe[c] | $E_0$(A) | $1.834 \pm 0.003$ | $4.24 \pm 0.2$ | $118 \pm 40$ | $36 \pm 5$ | $179 \pm 40$ |
| | $E_0$(B) | $1.860 \pm 0.002$ | $4.17 \pm 0.1$ | $93 \pm 20$ | $31 \pm 6$ | $152 \pm 25$ |
| | $E_0$(C) | $2.263 \pm 0.004$ | $3.96 \pm 0.2$ | $81 \pm 35$ | $27 \pm 8$ | $142 \pm 40$ |
| ZB-type ZnSe[d] | $E_0$ | $2.800 \pm 0.005$ | $7.3 \pm 0.4$ | $295 \pm 35$ | $73 \pm 4$ | $260 \pm 10$ |
| ZB-type $Zn_{0.56}Cd_{0.44}Se$[d] | $E_0$ | $2.267 \pm 0.004$ | $6.1 \pm 0.5$ | $206 \pm 35$ | $62 \pm 4$ | $236 \pm 10$ |

[a] Present work (contactless electroreflectance/photoreflectance).
[b] Reference [15] (contactless electroreflectance).
[c] Reference [13] (spectroscopic ellipsometry).
[d] Reference [16] (contactless electroreflectance).

The temperature dependence of the peak positions of the band-edge exciton features can also be described by a Bose–Einstein-type expression [13]

$$E_0^j(T) = E_0^j(0) - 2a_{B,j}/[\exp(\Theta_{B,j}/T) - 1], \tag{3}$$

where the index $j$ refers to either A or C exciton transitions, $E_0^j(0)$ is the transition energy at $T = 0$ K, $a_{B,j}$ represents the strength of the electron (exciton)–average phonon interaction, and $\Theta_{B,j}$ corresponds to the average phonon temperature. Shown by the dotted lines in figure 3 are least-squares fits to equation (3). The obtained values for the various parameters are also given in table 1. For comparison purposes, the parameters for the near-band-edge transition energies of WZ-type $Cd_{0.925}Be_{0.075}Se$ [15], WZ-type CdSe [13], ZB-type ZnSe [16], and ZB-type $Zn_{0.56}Cd_{0.44}Se$ [16] are also listed in table 1.

The parameter $\alpha_j$ of equation (2) can be related to $a_{B,j}$ and $\Theta_{B,j}$ in equation (3) by taking the high-temperature limit of both expressions. This yields $\alpha_j = 2a_{B,j}/\Theta_{B,j}$. Comparison of the numbers presented in table 1 shows that this relation is indeed satisfied. From equation (3), it is straightforward to show that high-temperature limit of the slope of the $E_0^j(T)$ versus $T$ curve approaches the value of $-2a_{B,j}/\Theta_{B,j}$. The calculated values of $-2a_B/\Theta_B$ for exciton A and exciton C equal $-0.40$ and $-0.42$ meV K$^{-1}$ respectively, which agree well with the value of $[dE_0^{A(C)}(T)/dT] = -0.40$ and $-0.41$ meV K$^{-1}$ as obtained from the linear extrapolation of the high-temperature (300–400 K) CER/PR experimental data.

The experimental values of the temperature dependence of the linewidth $\Gamma(T)$ of the fundamental band edge exciton A obtained by CER/PR measurements are displayed in figure 4 for a WZ-type $Cd_{0.85}Mg_{0.15}Se$ mixed crystal. Initially, $\Gamma(T)$ increases linearly with $T$, but it begins to be superlinear starting from about 150 K. The temperature dependence of the linewidth of excitonic transitions of semiconductors can be expressed as [17]

$$\Gamma(T) = \Gamma(0) + \gamma_{AC}T + \frac{\Gamma_{LO}}{[\exp(\Theta_{LO}/T) - 1]}. \tag{4}$$

In equation (4), $\Gamma(0)$ represents the broadening invoked from temperature-independent mechanisms, such as electron–electron interaction, impurity, dislocation, and alloy scattering, whereas the second term corresponds to lifetime broadening due to the exciton–acoustical

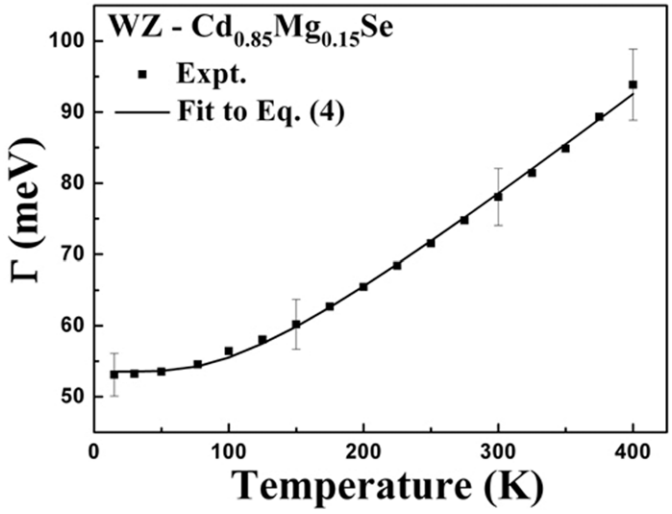


**Figure 4.** Temperature dependence of the linewidth $\Gamma(T)$ for exciton A of a WZ-type $Cd_{0.85}Mg_{0.15}Se$ mixed crystal with representative error bars. The full curve is a least-squares fit to equation (4).

**Table 2.** Values of the parameters that describe the temperature dependence of the broadening function $\Gamma$ for exciton A of a WZ-type $Cd_{0.85}Mg_{0.15}Se$ mixed crystal. The parameters for WZ-type $Cd_{0.925}Be_{0.075}Se$, WZ-type CdSe, ZB-type ZnSe, and ZB-type $Zn_{0.56}Cd_{0.44}Se$ are included for comparison.

| Material | Feature | $\Gamma(0)$ (meV) | $\Gamma_{LO}$ (meV) | $\Theta_{LO}$ (K) | $\gamma_{AC}$ ($\mu$eV K$^{-1}$) |
|---|---|---|---|---|---|
| WZ-type $Cd_{0.85}Mg_{0.15}Se$[a] | $E_0$(A) | $54 \pm 4$ | $57 \pm 8$ | $370 \pm 80$ | $2 \pm 1$ |
| WZ-type $Cd_{0.925}Be_{0.075}Se$[b] | $E_0$(A) | $19 \pm 2$ | $50 \pm 5$ | $310 \pm 40$ | $2 \pm 1$ |
| WZ-type CdSe[c] | $E_0$(A) | $2.3 \pm 0.3$ | $23 \pm 1$ | 300[e] | |
| | $E_0$(B) | $4 \pm 1$ | $139 \pm 25$ | $775 \pm 86$ | |
| ZB-type ZnSe[d] | $E_0$ | $6.5 \pm 2.5$ | $24 \pm 8$ | 360[e] | 2.0[e] |
| ZB-type $Zn_{0.56}Cd_{0.44}Se$[d] | $E_0$ | $6.0 \pm 2.0$ | $17 \pm 6$ | 334[e] | 1.1[e] |

[a] Present work (contactless electroreflectance/photoreflectance).
[b] Reference [15] (contactless electroreflectance).
[c] Reference [13] (spectroscopic ellipsometry).
[d] Reference [16] (contactless electroreflectance).
[e] A fixed parameter.

phonon interaction with $\gamma_{AC}$ being the acoustical phonon coupling constant. The third term is caused by the exciton–LO phonon (Fröhlich) interaction. The quantity $\Gamma_{LO}$ represents the strength of the exciton–LO phonon coupling while $\Theta_{LO}$ is the LO phonon temperature [13, 18]. The full curve in figure 4 is a least-squares fit to equation (4) to evaluate $\Gamma(0)$, $\Gamma_{LO}$, $\Theta_{LO}$ and $\gamma_{AC}$ for the A interband excitonic transition of a WZ-type $Cd_{0.85}Mg_{0.15}Se$ mixed crystal. The obtained values of $\Gamma(0)$, $\Gamma_{LO}$, $\Theta_{LO}$ and $\gamma_{AC}$ are listed in table 2. For comparison, the values of $\Gamma(0)$, $\Gamma_{LO}$, $\Theta_{LO}$ and $\gamma_{AC}$ for WZ-type $Cd_{0.925}Be_{0.075}Se$ [15], WZ-type CdSe [13], ZB-type ZnSe [16], and ZB-type $Zn_{0.56}Cd_{0.44}Se$ [16] from other works are also included in table 2. The value of $\Gamma(0)$ for the Mg-containing mixed crystal is much larger than those of Be-containing mixed crystal and Mg-free thin-film samples, due mainly to the poorer crystalline quality of the Mg-containing crystal. Actually it is not easy to grow high-quality Mg-incorporated II–

VI mixed crystal samples with uniformly distributed Mg contents. As shown in table 2, the fitted value of $\Gamma_{LO}$ for the Mg-containing sample is comparable with that for the Be-containing sample, and is larger than those of Mg-free samples. The larger value of $\Gamma_{LO}$ is presumably related to the higher effective longitudinal optical phonon energy of the Mg-containing sample. In addition, it is possible that a larger deformation potential interaction, which may account for a significant fraction of $\Gamma_{LO}$ in addition to the Fröhlich interaction, is responsible for the larger $\Gamma_{LO}$ for the Mg-containing CdSe.

## 4. Summary

In summary, the near band-edge transitions of a modified Bridgman-grown wurtzite-type $Cd_{0.85}Mg_{0.15}Se$ mixed crystal have been carried out by temperature-dependent CER/PR measurements in the temperature range 15–400 K. Room-temperature SPS has been used as a technique for checking the surface condition of the sample. The temperature dependence of excitons A and C has been analysed by the Varshni-type and Bose–Einstein-type expressions. The parameters extracted from both expressions by extending into the high-temperature regime are found to agree reasonably well. The parameters that describe the temperature dependence of the broadening function of the exciton A have also been studied. The value of $\Gamma(0)$ for the Mg-containing mixed crystal sample is much larger than those of the Be-containing mixed crystal and Mg-free thin films samples, indicating a poorer quality of the sample. The fitted value of $\Gamma_{LO}$ is larger than those of Mg-free samples. The larger value of $\Gamma_{LO}$ is related to the higher effective longitudinal optical phonon energy and the presence of a larger deformation potential interaction of the Mg-containing sample.

## Acknowledgment

PJH and YSH acknowledge the support of National Science Council of Taiwan under Project No. NSC 95-2221-E-011-171.

## References

[1] Phillips M C, Wang M W, Swenberg J F, McCaldin J O and McGill T C 1992 *Appl. Phys. Lett.* **61** 1962
[2] Firszt F, Męczyńska H, Sekulska B, Szatkowski J, Paszkowicz W and Kachniarz J 1995 *Semicond. Sci. Technol.* **10** 197
[3] Ferreira S O, Sitter H, Krump R, Faschinger W, Brunthaler G and Sadowski J T 1995 *Semicond. Sci. Technol.* **10** 489
[4] Gaines J M, Drenten R R, Haberern K W, Marshall T, Mensz P and Petruzzello J 1993 *Appl. Phys. Lett.* **62** 2462
[5] Spiegel R, Bacher G, Herz K, Forchel A, Litz T, Waag A and Landwehr G 1996 *Phys. Rev.* B **53** 4544
[6] Oh E, Parks C, Miotkowski I, Dean Sciacca M, Mayur A J and Ramdas A K 1993 *Phys. Rev.* B **48** 15040
[7] Jobst B, Hommel D, Lunz U, Gerhard T and Landwehr G 1996 *Appl. Phys. Lett.* **69** 97
[8] Wang M W, Phillips M C, Swenberg J F, Yu E T, McCaldin J O and McGill T C 1993 *J. Appl. Phys.* **73** 4660
[9] Firszt F, Łęgowski S, Męczyńska H, Szatkowski J, Paszkowicz W and Godwod K 2000 *J. Cryst. Growth* **184/185** 1335
[10] Firszt F, Wronkowska A A, Wronkowski A, Łęgowski S, Marasek A, Męczyńska H, Pawlak M, Paszkowicz W, Strzałkowski K and Zakrzewski J 2005 *Cryst. Res. Technol.* **40** 386
[11] Pollak F H and Shen H 1993 *Mater. Sci. Eng.* R **10** 275
[12] Huang Y S and Pollak F H 2005 *Phys. Status Solidi* a **202** 1193
[13] Logothetidis S, Cardona M, Lautenschlager P and Garriga M 1986 *Phys. Rev.* B **34** 2458
[14] Varshni Y P 1967 *Physica (Utrecht)* **34** 149
[15] Huang P J, Huang Y S, Firszt F, Męczyńska H and Tiong K K 2006 *Solid State Commun.* **137** 82
[16] Malikova L, Krystek W, Pollak F H, Dai N, Cavus A and Tamargo M C 1996 *Phys. Rev.* B **54** 1819
[17] Lee J, Koteles E and Vassell M O 1986 *Phys. Rev.* B **33** 5512
[18] Lautenschlager P, Garriga M, Logothetidis S and Cardona M 1987 *Phys. Rev.* B **35** 9174